minerals

MDPI

Article

Potentially Toxic Elements in Ultramafic Soils: A Study from Metamorphic Ophiolites of the Voltri Massif (Western Alps, Italy)

Pietro Marescotti [1,*], Paola Comodi [2], Laura Crispini [1], Lara Gigli [3], Azzurra Zucchini [2] and Silvia Fornasaro [1]

1 DISTAV, University of Genova, C.so Europa, 26, I-16132 Genova, Italy
2 Dipartimento di Fisica e Geologia, University of Perugia, Piazza dell'Università, 1, I-06123 Perugia, Italy
3 Elettra Sincrotrone Trieste S.c.P.A., Strada Statale 14 km 163.5, I-34149 Basovizza, Italy
* Correspondence: pietro.marescotti@unige.it; Tel.: +39-345-0089181

Received: 17 July 2019; Accepted: 9 August 2019; Published: 20 August 2019

Abstract: Ultramafic soils are characterized by severe edaphic conditions induced by a low content of essential nutrients, an adverse Ca/Mg ratio, a low water-holding capacity, and high contents of geogenic potentially toxic elements (PTEs), in particular Cr, Ni, and Co. These metals commonly exceed the content limits set by environmental agencies and governments, representing serious environmental risks for ecosystems and human health. In alpine environments, ultramafic soils are characterized by modest thickness and poor horizon differentiation. Several studies on ultramafic soils have shown that their properties may be directly related to the characteristics of the parent rocks, but most of these studies deal with soil chemistry, metal availability, isotopic composition, and pedological characterization. The aim of this research is to investigate how much the geotectonic characteristics of ultramafic bedrocks, such as the degree of serpentinization, metamorphic imprint, and deformation, may affect the mineralogical and chemical variations of ultramafic soils, including the occurrence and potential mobility of the PTEs. Using a multiscale and multi-analytical approach, we fully characterize the properties and mineralogical composition of soil profiles with different ultramafic parent rocks, i.e., partially serpentinized peridotite, massive serpentinites, and foliated serpentinites, sampled within the Voltri Massif High Pressure–Low Temperature (HP–LT) metaophiolite (Western Alps, Italy). Our results, related to soils located at comparable latitude, altitude, landscape position, and pedological environment, outline that the degree of serpentinization, the metamorphic imprint, and the deformation history of the ultramafic parent rocks are key factors influencing soil evolution, mineralogy, and chemistry, as well as PTEs distribution and mobility. Moreover, this study shows that the high content of Cr, Ni, and Co in the studied ultramafic soils has to be considered of geogenic origin and highlights the need for new approaches and methods to obtain indications on the potential contamination of natural or anthropogenic soils.

Keywords: peridotite soil; serpentine soil; Voltri Massif; LA–ICP–MS; ELETTRA Synchrotron Radiation Facilities; trace elements

1. Introduction

Ultramafic soils developed on peridotite and serpentinite bedrocks are characterized by severe edaphic conditions mainly induced by the (i) low content of essential nutrients (e.g., Ca, K, P, N), (ii) adverse Ca/Mg ratio, (iii) low water holding capacity, and (iv) high contents of geogenic potentially toxic elements (PTEs), in particular Cr, Ni, and Co [1–9]. These metals commonly exceed, by up to one order of magnitude, the content limits laid down by environmental agencies and governments [7,10,11], thus posing several environmental threats for ecosystems and human health [12,13].

Although ultramafic soils occur worldwide in almost all of the 12 orders [14], it is known that most such soils reach a limited development stage, especially in cold and temperate climatic conditions such as alpine environments [15]. In fact, in these environments, ultramafic soils are commonly characterized by modest thickness and poor horizon differentiation (lithosols, regosols, and rankers) [5,16–18]. They are also defined as "AC soils" because the O horizon is commonly absent or a few millimeters thick and the poorly developed A horizon is directly in contact with the C horizon [9,19].

The bedrock type is the most important factor influencing the mineralogical, geochemical, micromorphological, and pedological properties of these poorly developed soils [5,9,10,20–24]. In particular, although ultramafic soils are commonly grouped together under the term "serpentine soils" [22], significant differences can be present in soils derived from non- or slightly-serpentinized peridotites, massive serpentinites, metamorphic serpentine schists, and fractured or veined serpentinites. These differences can affect the soil chroma, depth, and weathering intensity as well as the nature and relative abundance of primary residual minerals and newly formed authigenic phases [1,15,22,23,25–29].

The aim of this article is to investigate how different degrees of serpentinization, metamorphic imprint, and deformation affect the mineralogical and chemical variations occurring in ultramafic soils, as well as the influence of the primary and authigenic mineral phases on the occurrence and potential mobility of PTEs (particularly Cr, Ni, and Co).

As a case study, we selected three different soil types from the Voltri Massif meta-ophiolite (W-Alps, NW Italy), which is characterized by a wide variety of peridotite and serpentinite that were involved in various different tectonic and metamorphic events.

From our results, we can envisage the potential environmental hazard of the PTEs contents in natural ultramafic soils with different backgrounds, also taking in account the actual threshold limits for PTEs laid down by international and national agencies.

2. Geological Setting

The study area is located in the Voltri Massif (VM), which is a metamorphic ophiolite complex with sedimentary cover, located at the southernmost tip of the arc of the Western Alps (Italy; Figure 1). The VM is considered a relic of the Jurassic Ligurian Tethys and is composed of HP–LT units accreted during the Late Mesozoic to Cenozoic Alpine orogeny ([30] and references therein).

The VM is mainly composed of ultramafic rocks (peridotite and serpentinite), mafic rocks (metagabbro and metabasalt), and calcschists with a polyphase tectonic and metamorphic imprint, from eclogite and blueschist facies prograde peak to retrograde greenschist facies [30–37].

Ultramafic rocks are the main lithology in the VM and are either mantle peridotite form subcontinental lithospheric (Erro–Tobbio Peridotite *Auct*) or oceanic crust serpentinites [30,33,36,38,39].

In places, peridotites occur as km- to m-scale bodies within serpentinites and mainly consist of spinel- and plagioclase-bearing lherzolite, with minor harzburgite, dunite lenses, and pyroxenite bands. They have been partially serpentinized during the oceanization and recrystallized to various degrees during the HP–LT events of the Alpine orogeny ([30,37] and references therein). Locally, peridotites still preserve textures and mineralogical associations of the pre-Alpine mantle evolution that includes olivines, ortho- and clino-pyroxenes, spinels, and plagioclases [30,38]. The ocean-floor metamorphism produced the partial replacement of the original mantle assemblages with mesh-textured antigorite, minor chrysotile (after olivine), bastites and/or Mg-rich amphiboles (after pyroxenes), magnetite (after spinels), and chlorite [39].

Oceanic serpentinites are antigorite-bearing serpentinites and serpentine schists, with rare textural relics of the original peridotite. Serpentinites are commonly characterized by a pervasive composite schistosity, with superposed phases of folds and shear bands [36,37,40–43]. In antigorite-bearing serpentine schists, the main foliation is commonly defined by antigorite, chlorites, and magnetite [31,44]. At the contact between serpentinites and other lithologies (e.g., metasediments and metabasites),

levels or rims of "hybrid rocks" [45] (composed of chlorite, talc, tremolite, actinolite, albite, titanite, and magnetite) frequently occur with various thickness (centimetric to plurimetric scale) and degree of deformation [35,36].

Ultramafic soils of the Voltri Massif are poorly investigated and are mostly classified as Lithic or Episkeletic Leptosols or, subordinately, Mollic Leptosols, with limited profile differentiation, continuous weathered bedrock close to the surface, and weakly developed O and A horizons [16,46–48].

The study area has a temperate oceanic climate with mean annual precipitation ranging from 1000 to 1400 mm/years and mean annual temperatures from 9.1 °C to 10.2 °C [47].

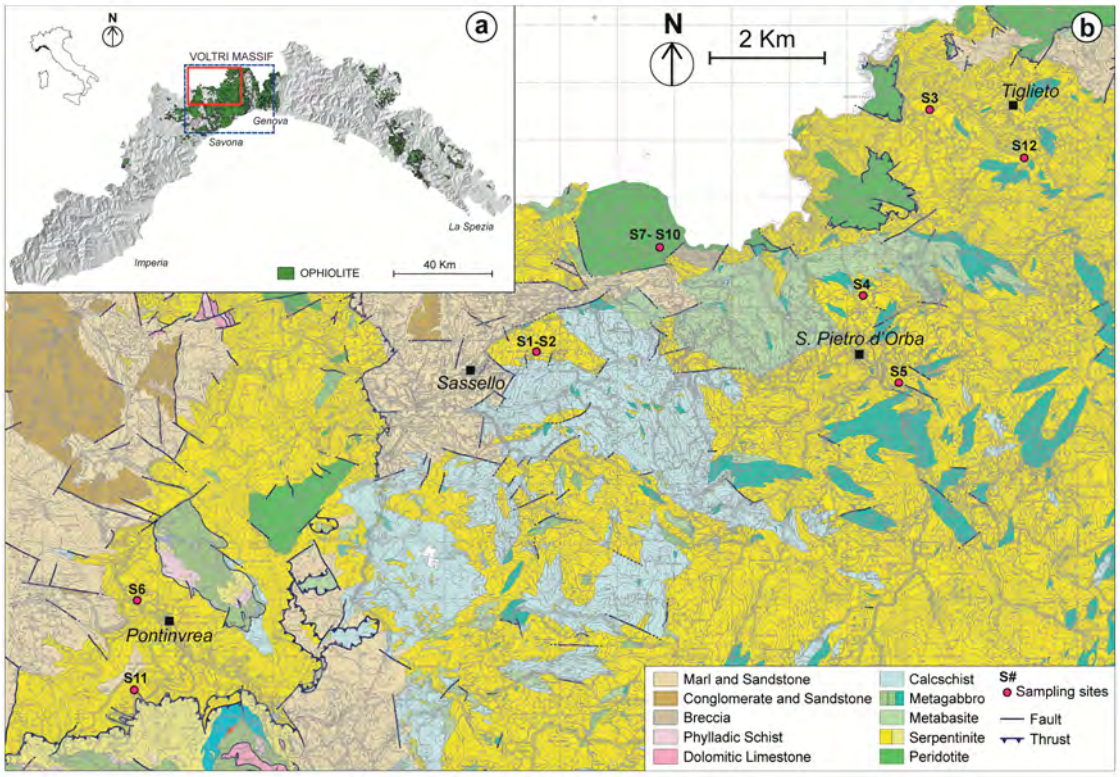

Figure 1. (**a**) Location of the study area (red box) within the Voltri Massif (Blue dashed box). Map supplied as Open Data by the Liguria Regional Government [49]. (**b**) Geological map of the study area with the sampling sites location (red dots); modified after [50]. Geographical information on sites S1-S12 is reported in Table S1.

3. Materials and Methods

Twelve soil profiles were sampled in eight sites within the VM ophiolite (Figures 1 and 2; Table S1), characterized by different ultramafic parent rocks, i.e., partially serpentinized lherzolites (PSP), massive serpentinites (MS), and foliated serpentinites (FS) (Figure 1b). In each site, approximately 1 kg of soil was collected from two layers following the criteria of GEMAS project [51]: (1) the topsoil (0–30 cm), excluding the rhizosphere, and (2) the subsoil (30–60 cm). The samples were collected with steel auger and shovel and sealed in plastic bags, after removing the granulometric fraction >2 cm.

The soil specimens were analyzed using a multiscale and multi-analytical approach.

(i) Soil properties including color, grain size, grain morphology, and structure were determined both in situ and in the laboratory and used to distinguish the soil horizons as well as to group soils according to the FAO–WRB classification [52]. The color was determined using the Munsell® Soil Color Charts [53]. The particle size distribution of all soil samples was obtained by wet sieving and granulometric classification was obtained according to the Folk and Shepard classifications [54,55].

(ii) Micromorphological analyses for qualitative weathering evaluation [56,57] and preliminary mineralogical/petrographic determination of soil samples were carried out using polarized-light

optical microscopy (PLOM) and scanning electron microscopy and microanalysis (SEM–EDS) at the Department for the Earth, Environment, and Life Sciences (DiSTAV), University of Genova, Italy.

The PLOM analyses were carried out using the BX-41 Olympus Microscope equipped with 2×, 4×, 10×, 20×, 40×, 50× objective magnifications and 10× and 12.5× eyepieces.

SEM investigations were performed using a SEM Vega3—TESCAN type LMU system equipped with an EDS EDAX APOLLO XSDD and a DPP3 analyzer. EDS analyses were collected at 20 kV accelerating voltage and 1.2 nA beam current at the specimen level for 60 live second counting time with a spot size of 370 nm and a working distance of 15 mm. Contents of major and minor elements were calculated on an anhydrous basis with ZAF corrections and using natural silicates and oxides for calibration.

(iii) Bulk chemical analyses were assessed by means of energy-dispersive X-ray fluorescence (EDXRF) using the X-MET7500 (Oxford Instruments) spectrometer (GeoSpectra s.r.l.—Spin-Off company of the University of Genova) and by inductively coupled plasma-atomic emission spectrometry (ICP–AES) at the Regional Agency for Environmental Protection of Liguria (ARPAL, Genova, Italy), using a Perkin Elmer–Optima 2100 DV spectrometer, on 3.5 g sample powder after total digestion of the material by melting with aqua regia (1 cc HNO_3 + 2 cc HCl).

(iv) Mineralogical analyses of three different granulometric fractions (sand fraction: 2 mm–63 μm; silt fraction: 63–2 μm, and clay fraction: <2 μm) were carried out by means of Synchrotron X-ray powder diffraction (XRPD) at the MCX beamline at Elettra Sincrotrone, Trieste, Italy [58]. Data were collected in transmission mode in the 2–70° 2θ range with different step size, 0.01 (sand and silt) and 0.005 (clay) and 1 s exposure time. A monochromatic wavelength of 1.033 Å (12 KeV) and 1 × 0.3 mm^2 spot size was used. The powder samples were loaded and packed in a 0.3 mm boron capillary, mounted on a standard goniometric head, and spun during data collection. Preliminary identification of mineral species was carried out with X'Pert Highscore, PDF-4+/Minerals, and Match! (PANalytical, Almelo, The Netherlands) software. For the quantitative analyses, Rietveld refinements were performed with General Structure Analysis software (EXPGUI–GSAS) [59–62] using the crystallographic information file (CIF) from the American Mineralogist Crystal Structure Database [63].

In order to check the amorphous content in the analyzed samples, the external standard method was used [64]. A constant amount of 10 wt % of metallic Si (99.5% metal-based powdered crystalline Silicon, 325 mesh, from Alfa Aesar, (Thermo Fisher Scientific, Kandel, Germany) was added to the powders obtained from the samples.

The composition of the clay fraction was analyzed after the granulometric separation of the fraction < 2 μm. For granulometric separation and treatments of clay fraction, the procedure reported in [65] was followed. Two oriented samples for each specimen were prepared to collect XRPD data on both the untreated and the treated (glycolated and thermal treated) materials and for each specimen, three XRPD patterns were collected: (a) untreated sample, (b) glycolated sample and (c) heated sample, at 335 °C for 4 h. The diffraction patterns were collected at the Department of Physics and Geology of the University of Perugia by means of a Philips PW-1830 diffractometer in Bragg-Bentano geometry with a monochromator on the exit signals and Cu K_α radiation (λ = 1.5406 Å). The qualitative analysis of the mineralogical clay composition was performed by comparing, for each specimen, the untreated, the glycolated, and the heated patterns using X'Pert Highscore software.

The mineral chemistry (major, minor and trace elements) were determined either by an Electron MicroProbe Analyzer (EMPA–WDS) or by in situ laser ablation–inductively coupled plasma–mass spectrometry (LA–ICP–MS).

EMPA–WDS analyses were carried out at the Electron Microprobe Laboratory of Earth Science Department "Ardito Desio" (University of Milan, Italy) using the EMPA–WDS JEOL 8200 Super Probe with the following operating conditions: accelerating voltage, 15 kV; beam current, 5 nA; counting time, 10 s for all the elements. Calibration for chemical analysis was accomplished with a set of synthetic and natural standards, including olivine (Mg), omphacite (Na), Cr, rhodonite (Mn and Zn), k-feldspar (K), anorthite (Al and Ca), wollastonite (Si), V, fayalite (Fe), ilmenite (Ti), Co, galena (S), and niccolite (Ni).

LA–ICP–MS analyses were carried out at the Department of Physics and Geology at the University of Perugia, Italy using a Thermo Fisher Scientific iCAP Q quadrupole mass spectrometer coupled with a Teledyne/Photon Machine ArF Excimer G2 laser ablation system (Teledyne CETAC Technologies Inc., Omaha, [NE], USA). The analyses were conducted using a ~30–20 µm beam diameter, 8 Hz frequency, and 0.032–0.105 mJ/pulse power, during 90 s analysis (50 s for the gas blank and 40 s on the grain). Details on the working conditions, instrumentation, precision, and accuracy are reported in Petrelli et al. [66].

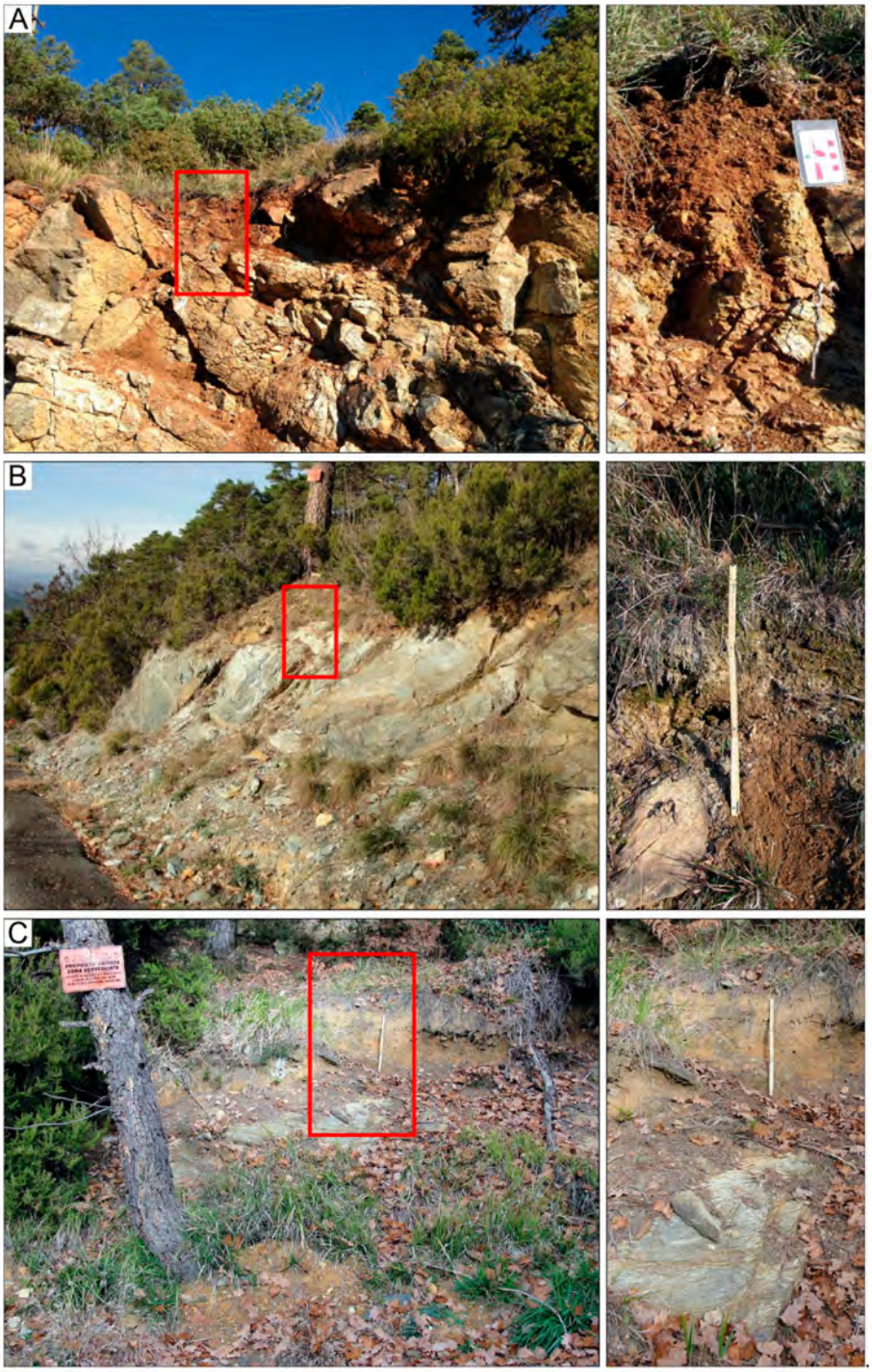

Figure 2. Representative photographs of the sampled sites. The red boxes indicates the sampled soil profiles shown on photographs to the right. (**A**) Soil profile on PSP bedrock (Site S7); (**B**) soil profile on MS bedrock (Site S2); (**C**) soil profile on FS bedrock (Site S1).

4. Results

4.1. Soil Profiles

Soil profiles on the three different ultramafic bedrocks (PSP, MS, and FS; Figure 2) are shallow to moderately deep (40–100 cm) and are generally characterized by a weakly developed A horizon, which is directly in contact with the C horizon, and a very thin O horizon (5–10 cm; Figures 2 and 3). However, the profile thickness slightly changes according to the different bedrock showing a systematic increase from PSP (40–60 cm; Figure 3a) toward MS (50–70 cm; Figure 3b) and FS (80–100 cm; Figure 3c). Cobbles and boulders are common throughout the entire profiles.

Soils on peridotites (PSP) were classified as Chromic Magnesic Leptic Skeletic Cambisols, whereas those developed on serpentinite bedrocks (MS and FS) were classified as Magnesic Leptic Skeletic Cambisols [60].

All the soil samples display heterogeneous granulometry without evident correlations with the bedrock types (Figure S1; Table S2); the topsoils were classified according to Folk's classification [54] as muddy-gravel, whereas the subsoils were classified as gravelly mud to gravelly sand. Soils show a relatively uniform particle size distribution in the gravely and sandy fractions, whereas the silty fraction is quite well sorted. The clay fraction is always a subordinate component in both topsoil and subsoil samples, varying from 7 to 2 wt %, respectively, with the highest values recorded in the topsoils of PSP and FS (5–7 wt %).

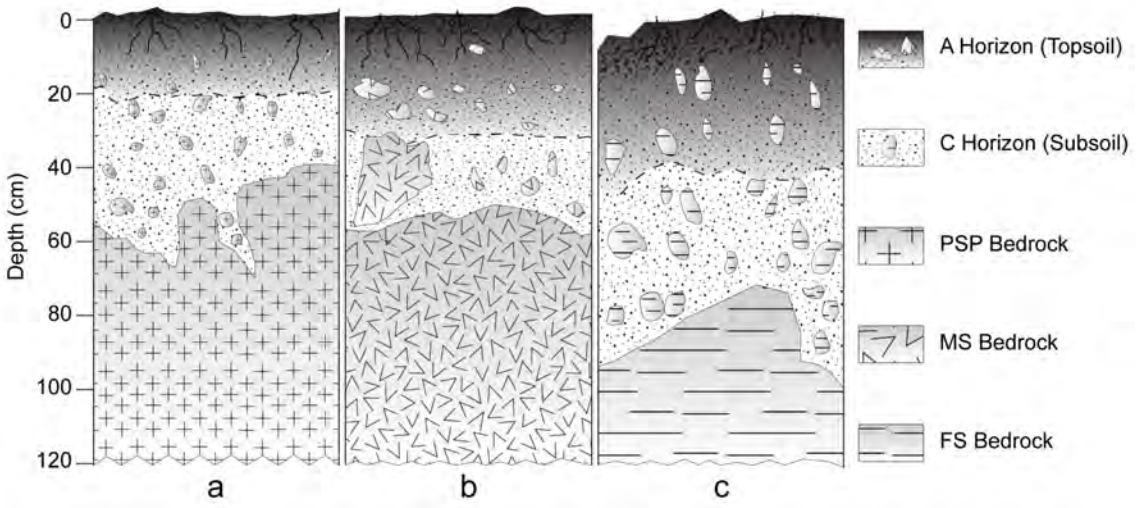

Figure 3. Schematic sketch of soil profiles developed on: (**a**) PSP; (**b**) MS; (**c**) FS. The dashed black lines represent the contact between A and C horizons.

The organic matter is mostly concentrated in the O horizon and at the top of the A horizon, where it varies from 20 to 29 wt % in MS and from 30 to 38 wt % in PSP and FS soils.

Contrary to the grain size, the color of the soils is clearly related to the variation in parent rocks (Table S2): (i) soils on PSP bedrock vary in color from "brown" (A horizon: 7.5 YR 5/4) to "reddish brown" (C horizon: 2.5 YR 5/4); (ii) soils on MS bedrock range from "dark brown" (A horizon: 10 YR 3/3) to "yellowish brown" (C horizon: 10 YR 5/4); (iii) soils on FS bedrock showed the most significant hue differences, varying from "dark yellowish-brown" (A horizon: 10 YR 4/6) to "greenish grey" (C horizon: Gley 1 5/1).

At the contact with the subsoil (C horizon), the bedrock of the studied soil profiles is variably weathered. However, the characteristics and the thickness of the weathering zone (1–10 cm) are influenced by the bedrock type, being the weathering intensity of PSP bedrock generally higher than those observed in MS and FS.

The PSP bedrock is typically capped by weathering rinds of up to 10 cm in thickness. These rinds are reddish brown to orange in color and are characterized by knobby relief marked by unaltered or weakly altered pyroxene highs (up to 15 mm in size) and strongly weathered olivine lows. Spinel-group minerals (up to 5 mm in size) generally appear unaltered, without any evidence of weathering reactions. The weathering rind is separate from the unweathered rock by sharp and irregularly undulated interface, though reddish oxidation halos commonly extend into the unaltered rock, around microfractures, the grain boundary, or intergranular porosity.

The MS bedrock is generally slightly altered and the rock surface has a characteristic dark green to olive green color. Evidence of incipient alteration was found only along fractures, where centimetric oxidation halos are commonly present. Moreover, scattered yellowish-red oxidation patches are present around magnetite aggregates.

The FS bedrock is moderately to weakly weathered and varies in color from green to greenish gray. Millimetric to centimetric ochreous-reddish oxidation halos developed around fractures and joints or along foliation planes.

4.2. Soil Micromorphology

Micromorphological analyses where performed to evaluate the weathering intensity based on the alteration patterns that characterize the soil skeleton clasts. Five main classes were recognized (Figure S2): (i) lithorelics, (ii) alterorelics, (iii) alteromorphs, (iv) iron crusts and nodules, and (v) allochthonous clasts.

Lithorelics, i.e., residual fragments of non-weathered parent rocks [56], represent the main components of the soil skeleton in all of the soil types and generally slightly decrease form subsoils toward topsoils. The modal abundance of lithorelics corresponds to approximately 70% in the C horizon of MS and decreases down to 60% and 40% in those of FS and PSP, respectively. The most common lithorelics in all of the studied soil samples are the serpentinite clasts, characterized both by pseudomorphic (PSP and MS) and non-pseudomorphic textures (FS and MS). Other common lithorelics are represented by monomineralic and polymineralic clasts, composed of spinel-group minerals, chrysotile, clinochlore, quartz, and pyroxenes.

Alteromorphs clasts have variable sphericity and generally low roundness, consisting of partially to completely weathered primary minerals and mostly preserving the primary textures. The most common alteromorphs are represented by serpentinite clasts, which are partially replaced by alteration products, mainly consisting of Fe oxyhydroxides, clay minerals, and iddingsitic mixtures. The modal abundance of alteromorphs is higher in soils developed on PSP bedrock (20%) than in those on MS and FS bedrocks (about 15%) and generally increases from the C toward the A horizon.

Alterorelics are highly weathered clasts with variable sphericity and generally medium to high roundness. These clasts are almost completely composed by authigenic minerals, mostly represented by Fe oxides (hematite), Fe oxyhydroxides, and iddingsitic mixtures replacing magnetite crystals and aggregates filling fractures and porosities. The modal abundance of alterorelics varies from 5% (FS) to 7% (MS) to 10–15% (PSP) with no significant difference between the A and C horizons.

Iron crusts and nodules are exclusively composed of Fe-oxyhydroxides and develop due to (i) precipitation around clast edges according to peripheral cortification process (in this case the clast cores are commonly preserved due to a shield effect) and (ii) precipitation within soil porosity giving rise to a concentric layering. The modal abundance of iron crusts is generally low (<5%), reaches the maximum value in soils on PSP bedrock, and slightly increases from the C toward the A horizon.

Allochthonous clasts are present in minor to trace amounts in all soil types and mostly occur in the topsoil horizons. They are mainly represented by quartz crystals or subangular polycrystalline quartz aggregates. Locally, close to tremolite-chlorite hybrid rock outcrops, amphibole-rich clasts occur in A horizons.

4.3. Soil Mineralogy

The results of the Rietveld refinement of the analyzed samples indicated that the soil profiles developed on the three different bedrocks (PSP, MS, and FS) are characterized by significant mineralogical variations, both for the main primary and authigenic mineral species and for their relative abundances (Table 1; Figure 4). Conversely, the mineralogical variations between the A horizon and the C horizon are less important and mainly concern the relative abundance between primary minerals inherited from the parent rocks and the newly formed authigenic minerals. Serpentine-group minerals (antigorite with minor chrysotile) are by far the most common primary minerals in all of the soil types, followed by clinochlore and spinel-group minerals. The spinels in soils on PSP (Cr-spinel, ferrian chromite, and Cr-magnetite) have a higher content with respect to those on MS (Cr-magnetite and magnetite) and, particularly, on FS (magnetite). Orthopyroxenes are present in non-negligible amounts only within soils on PSP (Table 1).

Table 1. Mineralogy of soils on PSP, MS and FS, resulted from Synchrotron Radiation XRPD analyses and Rietveld refinement, and of the separated clay fraction (<2 μm) after glycolation and thermal treatment. Data (expressed in weight percentage—wt %) represent the mean (three samples) resulting from the recalculations of the values obtained in the three grain-size fractions (sand, silt, and clay fractions). Accessory minerals were recognized by SEM–EDS and EMPA–WDS analyses. The sum of the primary and authigenic minerals is reported at the bottom of the table. Primary minerals include Atg, Clc, Spl, Ctl, and En, whereas authigenic minerals include Gt, clay minerals, amorphous and/or low crystalline phases.

Bedrock Type	**PSP**		**MS**		**FS**	
	A horizon	**C horizon**	**A horizon**	**C horizon**	**A horizon**	**C horizon**
Antigorite	43.1	48.1	52.1	56.4	50.8	57.2
Clinochlore	9.8	15.7	5.4	12.6	1.6	4.5
Spinel-group minerals	8.6	8.3	5.4	6.8	0.9	7
Chrysotile	2.2	2.1	2.7	2.9	0.9	2
Enstatite	8.3	9.1	n.d.	n.d.	n.d.	n.d.
Goethite	4.3	4.8	n.d.	n.d.	0.9	0.7
Clay minerals	2.8	0.8	2.7	2.2	8.7	5.2
Amorphous	20.9	11.2	31.9	19.1	36.2	23.3
Accessory Minerals	Hem, Tr, Ol, Aug, Qtz, Cal	Hem, Tr, Ol, Aug, Pl, Qtz	Hem, Gt, Tr, Rt, Ilm, Hl, Qtz	Pl, Gt, Hem, Qtz	Tlc, Rt, Hem, Cal, Qtz	Tlc, Hem, Qtz
Primary minerals	72	83.2	65.5	78.7	54.2	70.8
Authigenic minerals	28	16.8	34.5	21.3	45.8	29.2
Refinement details						
Rp	0.071	0.073	0.071	0.079	0.086	0.087
Rwp	0.101	0.100	0.091	0.101	0.110	1.123
Mineralogy of the clay fraction						
	Atg, Ol, Qtz, Chl*	Atg, Ol, Hem, Chl*	Atg, Qtz, Ol, Chl*	Atg, Chl*, Qtz, Mag	Chl*, Ill, Qtz	Chl*, Qtz, Ill

Abbreviations: n.d.: not detected; Rp: unweighted-profile R-factor; Rwp: weighted-profile R-factor. Accessory mineral abbreviations after [67]. Chl* means low crystalline chlorite (see text).

Authigenic minerals content strongly increases from C toward A horizons in all of the studied profiles (Table 1). Most of these minerals occurs in the clayey fraction (<2 μm) and are mainly represented by amorphous and/or low crystalline phases, with subordinate clay minerals and goethite. Based on EPMA analyses, most of these amorphous phases are represented by Fe oxides and oxyhydroxides.

The highest content of authigenic minerals and amorphous phases invariably occurs in soils from FS bedrocks. Finally, calcite and halite commonly occur in minor amount in A horizon samples likely precipitating from the circulating water.

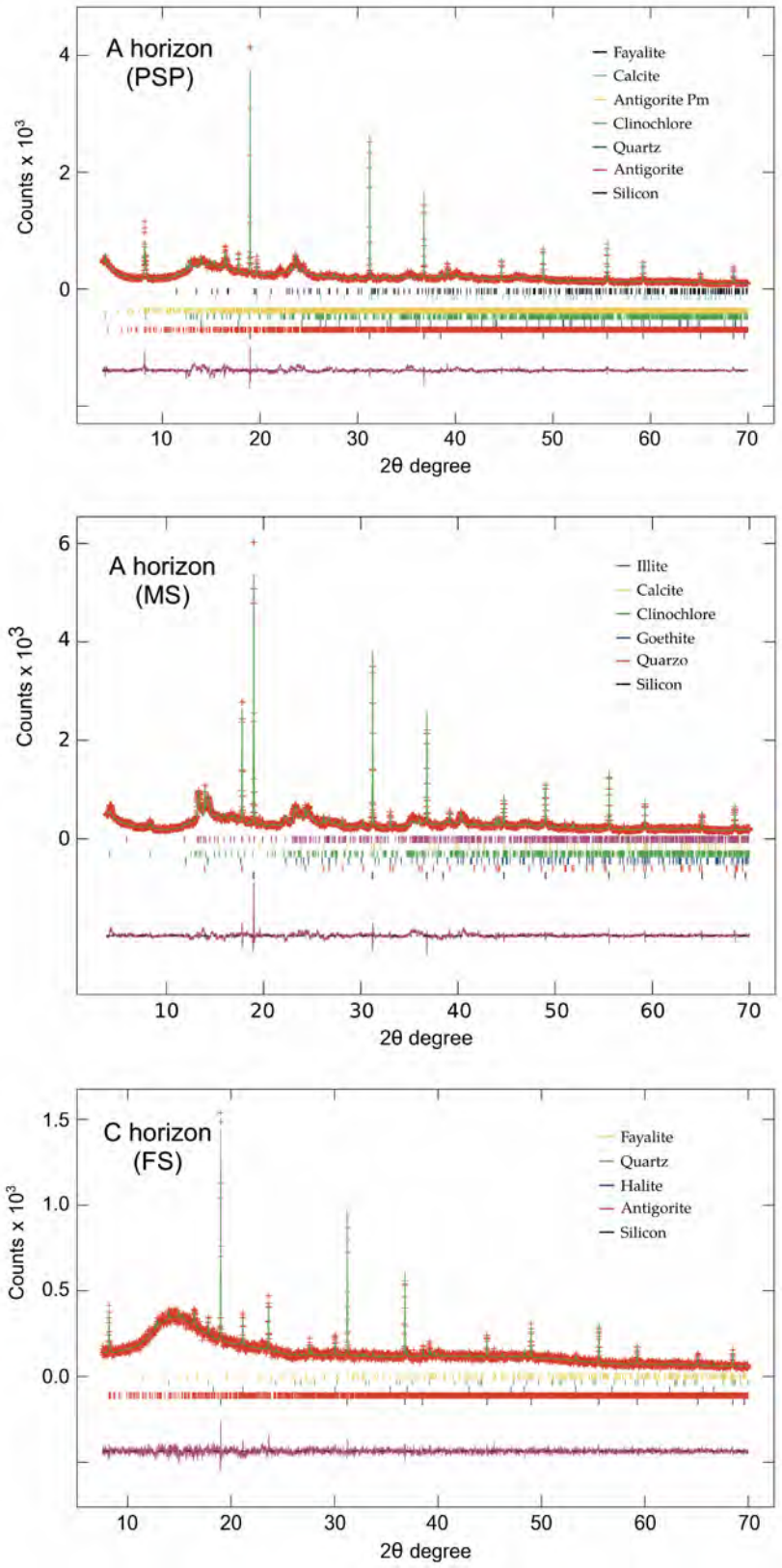

Figure 4. Refined XRPD patters of the silt fraction of representative samples. The red crosses are the observed data and the green profiles are the calculated pattern. The difference curve is shown in purple. Bars at the bottom of the graphs are the mineral phases reference diffraction peaks; see the legends to attribute colors to phases (from top to the bottom). Silicon is the internal standard added to the sample to determine the amorphous content.

In order to obtain a more definitive characterization of the clay fraction, glycolated and heated samples were also analyzed. As shown in Table 1, chlorite is the main clay mineral present in all of the soil types. We decided to named chlorite as low crystalline chlorite on the basis of the results of thermal treatment. Really the glycolated spectra indicate unswelling clays, and the peak positions are those of chlorite mineral. However, the disappearance of (001) reflection after thermal treatment at 335 °C indicates a very low thermal stability, anomalous for chlorite with a good crystallinity. Zanazzi et al. [68] showed the thermal stability of chlorite up to 550 °C by measuring the evolution of lattice parameters without relevant change in symmetry or de-hydroxylation phenomena.

Hematite is common only in C horizon of soils from PSP, whereas illite was identified only in soils from FS. Quartz is present in almost all of the analyzed samples; its origin is not clear since it could represent a newly formed mineral, be a relic of quartz veins (present in serpentinite), or have allochthonous origin. Even in the clay fraction, primary minerals inherited from the parent rocks are still present, mostly represented by antigorite. A small amount of olivine is also present in A horizons of soils from PSP and MS.

4.4. Bulk Chemistry

The three groups of ultramafic soils under investigation are characterized by significant variations in Mg and Si. In particular, the MgO/SiO_2 ratio systematically decreases from soils on PSP toward those on MS and FS (Table 2), in good agreement with the chemical variations observed in the bedrocks, which are characterized by a systematic decrease of the ratio with the increasing serpentinization degree [69]. Moreover, all soil types showed a significant decrease in the MgO/SiO_2 ratio upwards in the profiles due to both a progressive loss of Mg and an increase of Si during the soil evolution (Figure 5; Table 2). Iron slightly decreases from the C toward the A horizon in soils on PSP, whereas it remains almost unchanged in the other soil types (Figure 5).

Aluminum, calcium, manganese, and titanium are minor components of all soils and they are rather stable within the profiles of the different soil types (Table 2).

Studied soils contain elevated contents of PTEs, particularly Ni, Cr, and Co, in good agreement with the chemistry of the respective ultramafic parent rocks that were recently analyzed in the same sites by Fornasaro et al. [69] (Figure 6; Table 2).

Median nickel contents significantly decrease from bedrock [69] upwards in the profiles in all soil types, with the highest variation observed in soils on PSP (Table 2; Figure 6). Median chromium contents had a behavior similar to that observed for Ni in MS and FS soils, but an opposite trend was observed in soils on PSP (Figure 6), where Cr content greatly increases from bedrock (median value = 1260 ppm [69]) to soil profile, with a slight decrease from the C horizon (median value = 2330 ppm; Table 2) toward the A horizon (median value = 2100 ppm; Table 2).

Concerning median Co contents, no systematic trends resulted with respect to the soil type and depth and the observed chemical variations are generally lower than those observed for Ni and Cr. A slight increase from bedrock toward the A horizon resulted in soils on PSP, whereas soils on MS showed an opposite trend and those on FS remained almost unchanged (Table 2, Figure 6).

Vanadium, zinc, and copper are generally present in low contents, although anomalous high values were observed locally for zinc (i.e., more than 400 ppm in a soil profile on MS both in C and A horizons; Table 2). These three elements were rather stable within the profiles for all of the soil types.

Table 2. Chemical composition of the studied soils (Avg = average; M = median; Min = minimum; Max = maximum). Major and minor elements are reported as oxide wt %; selected PTEs are reported in ppm.

Type	Data	MgO	Al_2O_3	SiO_2	CaO	TiO_2	MnOt	FeOt	V	Cr	Co	Ni	Cu	Zn
Soils on PSP Bedrock														
A horizon	Avg	21.13	3.05	33.34	1.30	0.15	0.18	12.15	60	1940	130	1530	30	60
	M	21.27	3.05	34.60	1.25	0.15	0.18	11.99	70	2100	130	1670	30	80
	Min	17.91	2.64	29.01	0.67	0.12	0.17	10.15	30	960	60	1040	10	10
	Max	23.91	3.47	35.15	2.04	0.20	0.19	14.47	70	2400	170	2050	40	80
C horizon	Avg	22.64	2.66	32.71	1.06	0.12	0.20	14.65	60	2010	140	1850	20	50
	M	23.63	2.83	32.82	1.24	0.13	0.17	14.33	60	2330	130	1880	30	60
	Min	18.07	1.71	30.82	0.17	0.05	0.16	11.31	30	870	60	890	10	10
	Max	25.38	3.26	34.37	1.60	0.15	0.30	18.63	70	2480	260	3130	40	80
Soils on MS Bedrock														
A horizon	Avg	20.84	7.71	53.04	1.14	0.76	0.19	9.87	80	1290	110	710	20	150
	M	20.71	7.92	52.97	1.09	0.77	0.19	9.58	100	1460	110	860	20	80
	Min	15.90	6.24	51.14	0.97	0.69	0.16	9.53	10	620	30	270	10	70
	Max	26.03	8.75	55.07	1.41	0.83	0.22	10.79	140	1690	150	1050	30	430
C horizon	Avg	21.41	7.14	50.82	0.87	0.70	0.22	9.88	90	1840	190	1180	30	150
	M	21.41	6.99	49.82	0.88	0.71	0.22	9.85	100	2350	250	1140	20	70
	Min	14.30	6.79	48.23	0.46	0.32	0.22	9.27	30	660	30	290	10	50
	Max	28.52	7.79	55.42	1.27	1.04	0.22	10.54	130	2510	290	1890	80	480
Soils on FS Bedrock														
A horizon	Avg	16.58	9.46	54.53	1.28	0.92	0.25	10.87	80	1220	110	640	20	40
	M	17.08	9.46	54.53	1.28	0.92	0.25	10.93	80	1100	90	420	10	40
	Min	12.89	8.35	50.46	1.02	0.69	0.23	10.46	10	610	30	300	10	10
	Max	19.27	10.57	58.59	1.53	1.15	0.27	11.17	150	2080	210	1430	40	80
C horizon	Avg	19.80	8.82	50.90	1.18	1.08	0.34	14.05	90	1620	160	850	30	60
	M	19.80	8.82	50.85	1.18	1.08	0.37	14.05	70	1700	120	720	20	60
	Min	18.27	6.99	50.49	0.53	0.66	0.20	11.03	30	860	20	560	10	20
	Max	21.34	10.64	51.40	1.83	1.50	0.44	17.08	170	2200	370	1390	60	100

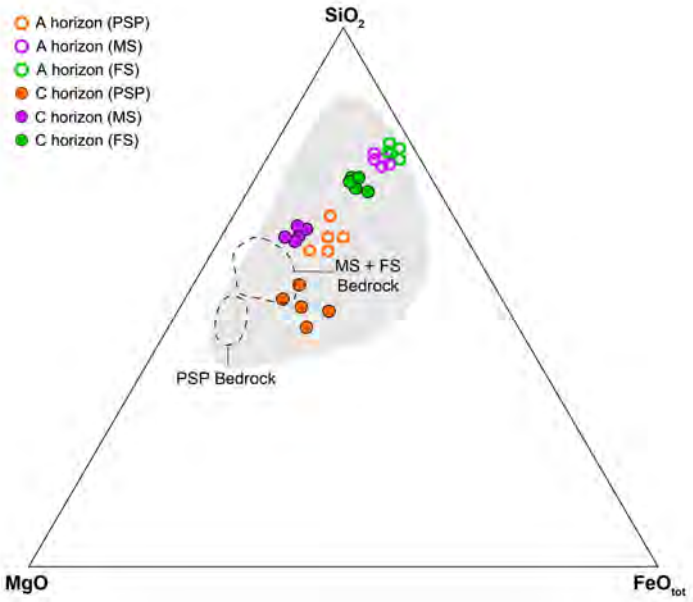

Figure 5. Ternary diagram of MgO–SiO_2–FeOtot for the studied soils. The gray field corresponds to the composition of ultramafic soils worldwide (data from [5,9,10,16,28,52,70–74]). Dashed fields correspond to the composition of bedrock of the studied soils (data from [69]).

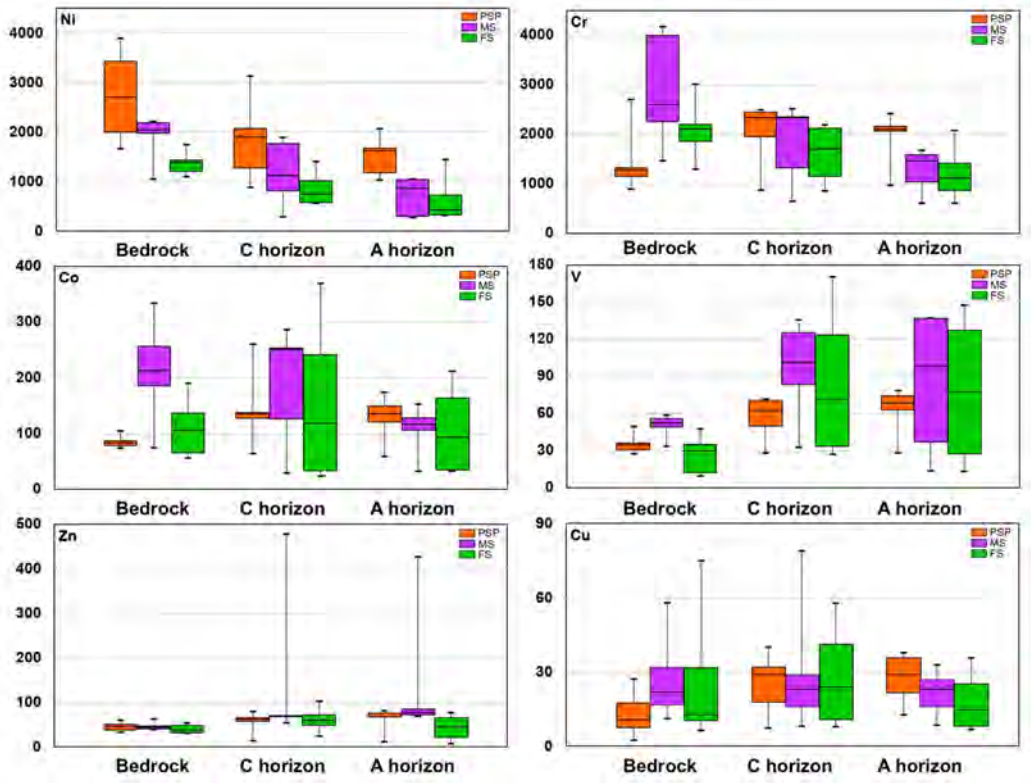

Figure 6. Box plots showing statistical parameters for contents (in ppm) of Ni, Cr, Co, V, Zn, and Cu in soils on PSP, MS, and FS bedrocks. Vertical lines show the range in contents, the boxes are bounded by the 1st and 3rd quartile whereas the horizontal line inside the box represents the median value. Statistical parameters are based on 30 analyses. Bedrock data from [69].

4.5. PTEs Distribution in Primary and Authigenic Minerals

The PTEs considered in this work (Ni, Cr, Co, V, Cu, and Zn) are hosted both in primary and authigenic minerals (Figure 7; Tables S3 and S4). Although some of these elements are present in high content in several minor to accessory minerals (e.g., nickel in olivine, talc, and Ni sulfides), the principal PTEs carriers are the volumetrically major constituents of the studied soils. Among these, spinel-group minerals, antigorite, and chlorite represent the most important PTEs bearing primary minerals, whereas low-crystalline to amorphous Fe oxyhydroxides and clay minerals are the main PTEs-bearing authigenic phases (Figure 7).

The principal Ni-bearing primary minerals in all soil types are spinel-group minerals (Cr-magnetite up to 3800 ppm, ferrian chromite up to 2317 ppm, and magnetite up to 3990 ppm), antigorite (up to 2614 ppm), and clinochlore (up to 2848 ppm). The most significant variations in Ni content were observed in antigorite from PSP soils (min: 255 ppm; max: 2614 ppm; median: 1764 ppm) with the lowest contents always associated to antigorite occurring in bastites after pyroxenes, whereas the highest contents are in the antigorite occurring in mesh and ribbon textures after olivine (Figure 7). The content of Ni in authigenic minerals is much more variable, depending both on soil type and mode of occurrence. The highest and more variable content was recorded in Fe oxyhydroxides, mostly represented by amorphous phases and crystalline goethite (Figure 7). The highest median contents were found in soils on PSP (4797 ppm), up to one order of magnitude higher than those in MS and FS. In these soils, the highest Ni content (3840 ppm and 3700 ppm, respectively) was recorded in Fe oxyhydroxides occurring within alteromorphs after magnetite and serpentinite clasts, as well as in alterorelics, whereas the lowest content generally occurs in iron nodules and iron crusts. Concerning the clay minerals, the variations in Ni contents are mostly related to the different mineral species with the highest contents (up to 3300 ppm) in low-crystalline chlorites and the lowest (down to 46 ppm) in illite.

Spinel-group minerals are, by far, the most important Cr-bearing primary minerals (Figure 4) in all of the studied soils being characterized by Cr contents varying from about 21 wt % (ferrian chromite) to about 17.5 wt % (Cr-magnetite), to 3.5 wt % (magnetite). The variations in the median values in the three soil types mostly depend on the relative abundance of magnetite with respect to ferrian chromite and Cr-magnetite, the latter being much less frequent in soils on MS and FS bedrocks.

Clinochlore generally has high Cr content in all of the soil types, with the highest median values in FS and PSP soils (3532 ppm and 3245 ppm respectively) and the lowest median values (1687 ppm) and the highest variability in soils on MS (Figure 7).

The Cr contents in antigorite are relatively high and homogeneous in soils on MS and FS (median values 2220 ppm and 2246 ppm, respectively); conversely, antigorite crystals occurring in soils on PSP are characterized by the lowest median values (466 ppm) but the highest variability.

High contents of Cr are also present in enstatite (median value 5368) although it occurs in significant amounts only in soils on PSP bedrock (Table 1).

Similarly to Ni, the content of Cr in authigenic minerals is much more variable depending both on soil type, mode of occurrence and mineralogy.

The highest and more variable contents were recorded also in this case in low crystalline to amorphous Fe oxyhydroxides (Figure 7) occurring in soils on PSP as alteromorphs after spinel-group minerals. Nevertheless, the very high median content (about 10 wt %) possibly suggest the presence of spinel relics intimately intermixed with the Fe oxyhydroxides. Also, in the other two soil types (MS and FS) the highest contents were found in alteromorphs after Cr-magnetite and magnetite.

In the clay minerals, the variations in Cr contents are mostly related to the different mineral species with the highest contents (up 4750 ppm) in low-crystalline chlorites and the lowest (down to 82 ppm) in illite. It is worth to note that the higher Cr contents systematically occur in clay minerals from soils on MS and FS were most of the spinel-group minerals are represented by magnetite, which is, generally, much more weathered than the ferrian chromite and Cr-magnetite occurring mostly in soils on PSP.

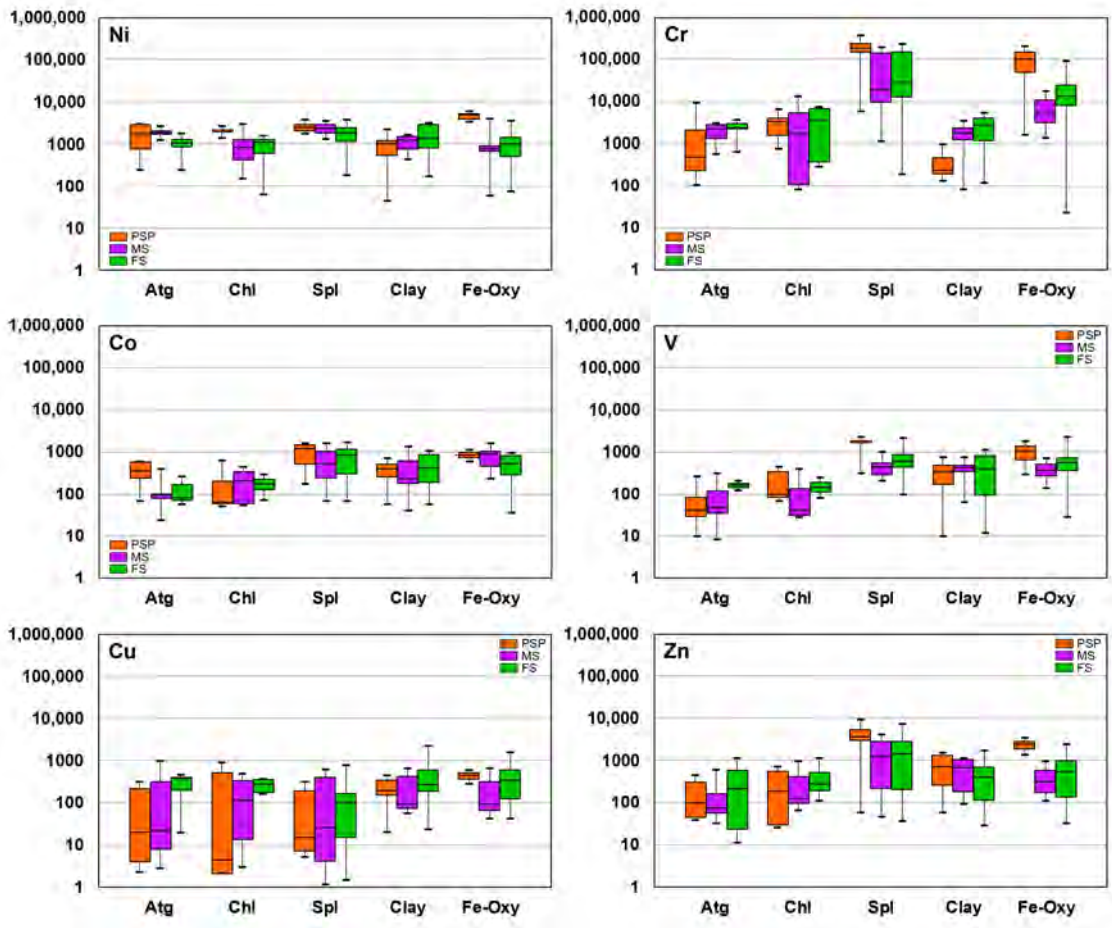

Figure 7. Box plots showing statistical parameters for contents (in ppm) of Ni, Cr, Co, V, Cu, and Zn in the main mineral species occurring in soils on PSP, MS, and FS bedrocks. Vertical lines show the range in contents, the boxes are bounded by the 1st and 3rd quartile, whereas the horizontal line inside the box represents the median value. Statistical parameters are based on the following number of analyses: Atg = 48; Chl = 23; Spl = 70; Clay = 52; Fe–Oxy = 85. Abbreviations: Atg: antigorite; Chl: clinochlore; Spl: spinel-group minerals; Clay: clay minerals; Fe-oxy: Fe oxyhydroxides. Within the Fe–Oxy class were both goethite and the amorphous Fe oxyhydroxides.

Among the primary minerals, spinels are the most important Co-bearing phases in all of the three soil types with median values ranging from 1214 ppm (soils on PSP) to 531 ppm (soils on MS). Antigorite and chlorite have relatively low Co contents; the highest median values (362 ppm) were recorded in antigorite occurring in pseudomorphic textures from soils on PSP and in chloritized pyroxenes from soils on MS and FS.

Also, in the authigenic minerals Co contents are generally much lower than Cr and Ni with the highest contents occurring in amorphous Fe oxyhydroxides and goethite (PSP).

As expected, the other PTEs (V, Cu, Zn) are generally present in primary minerals in lower contents than Cr, Ni, and Co. The only exceptions are represented by the spinel-group minerals (Figure 4), which are characterized by significantly high median contents of V (up to 1809 ppm) and Zn (up to 3675 ppm) in soils on PSP.

As for Cr, Ni, and Co, the authigenic minerals, both clay minerals and Fe oxyhydroxides, resulted to be able to sequestrate (presumably both through surface sorption as well as substitution) non-negligible amounts of PTEs. The highest median contents of V (1075 ppm), Cu (447 ppm), and Zn (3528 ppm) always occur in Fe oxyhydroxides alteromorphs and alterorelics in soils on PSP.

5. Discussion

The ultramafic soils studied in this work, which were developed on partially serpentinized peridotites (PSP), massive serpentinites (MS), and foliated serpentinites (FS), revealed significant differences in mineralogy, micromorphology, chemistry, and PTEs distribution. They represent the early stages of soil formation on different ultramafic rocks thus representing an important example of the mineralogical and chemical variations occurring during the initial phases of soil development in temperate climate.

Several studies on serpentinitic and ultramafic soils indicated that the soil properties as well as the variations in PTEs' distribution and bioavailability may be related to the different ultramafic parent rocks (i.e., serpentinites, peridotites, etc.). Most of these studies mainly deal with soil chemistry, metal availability based on chemical extraction procedures, phytoaccumulation investigations, isotopic composition, and pedological characterization (e.g., [23,29,73,75–80]). Only a few studies dealt with the implication of the different ultramafic parent rocks on the development of ultramafic soils and ecosystems, which is particularly important in young and poorly developed soil profiles (e.g., [9,28]).

Although climatic conditions, water regime, topography, and other soil forming factors play a pivotal role in the soil evolution and for their physicochemical properties, our results, related to soils located at comparable latitude, altitude, landscape position (i.e., at the top of slopes) and pedological environment, outline that the degree of serpentinization, the metamorphic imprint, and the deformation history of the ultramafic parent rocks are important factors influencing soil evolution, mineralogy, chemistry as well as PTEs distribution.

The mineralogical differences between the three types of soil concern both the authigenic and the primary minerals inherited by the parent rocks. The total amount of authigenic minerals increases significantly from soils on PSP (16.8–28 wt %) toward those on MS (21.3–34.5 wt %) and on FS (29.2–45.8 wt %) with the highest values always in the A horizon (Table 1). Among the authigenic minerals occurring in the clay fraction, amorphous and crystalline (only in PSP) Fe oxyhydroxides are, by far, the main mineral species occurring in all soil types. Clay minerals are subordinate constituents and they are mostly represented by *low crystalline chlorite* with minor illite in FS soils. Most of the iron comes from the weathering of primary silicates and, subordinately, of spinel-group minerals. The higher availability of iron in PSP during bedrock weathering can be explained by the higher weatherability of olivines and pyroxenes, which are present in significant amount only in PSP bedrocks [69], compared to antigorite, chrysotile, and chlorites, which are the main silicates in MS and FS bedrocks (e.g., [9,22,27,28,69]). This mineralogical framework explains the typical redder color of soils developed on PSP, which is a distinctive feature at the outcrop scale observed elsewhere (e.g., [14,22,25,27]). This hypothesis is also supported by the micromorphological analyses that have shown the highest quantities of Fe-bearing alteromorphs and alterorelics as well as iron crusts in soils on PSP.

The occurrence of chlorite as the main clay mineral in the clay fraction is in some ways surprising since smectites (in poorly drained soils) and vermiculites (in well-drained soils) are generally reported as the main clay mineral species in ultramafic soil toposequences (e.g., [1,9,15,26,28,46,77]. Nevertheless, the presence of "chlorite-like" pedogenic minerals has been already reported in ultramafic soils of the same area [46]. The presence of chlorite in the clay fraction has been considered as either the product of weathering of serpentine minerals or the pedogenic product deriving from the development of hydroxyinterlayers in smectites (e.g., [81]). Hseu et al. [24] suggest that similar non-expanding chlorite-like minerals on the clay fraction can be explained by the presence of randomly interstratified chlorite-vermiculite [21,82], i.e., a chlorite-like mineral with incomplete interlayer OH sheets. Randomly interstratified chlorite-vermiculite clay minerals have been also reported by Lee et al. [21] in an ultramafic soil toposequence from Trinity ophiolite, in the Klamath Mountains, California. Moreover, Bani et al. [77] and Istok and Harward [83] found smectite as the dominant clay mineral within poorly drained soils and chlorite in well-drained upland soils such as those of this study.

Among the primary minerals the fingerprint of the bedrock is more evident. As expected, antigorite is the main constituent in all of the soil types, whereas clinochlore is generally more abundant in PSP and MS. Particularly important, also from the environmental point of view, are the differences observed for the spinel-group minerals, both for their modal abundances and mineral species. The highest quantities were always observed in soils on PSP where they remain almost unchanged with depth. Conversely, the quantity of spinels significantly decreases from the bottom toward the top of the profiles of soils on MS and FS. This evidence can be explained by the fact that most of the spinels in PSP are represented by Cr-spinels, ferrian chromite, and Cr-magnetite, which are less weatherable than magnetite (e.g., [79]), the main spinel in MS and the only occurring spinel in FS.

The mineralogical differences between the three types of soil investigated in this work have a direct correlation with the soil chemistry and PTEs distribution. As resulted from EPMA and LA–ICP–MS analyses, the primary minerals, antigorite, spinel-group minerals, and clinochlore resulted, by far, in the most important PTEs-bearing phases (particularly Ni, Cr, and Co), as reported in several works dealing with serpentine and ultramafic soils (e.g., [10,28,69,77,84]). As concerns the authigenic minerals, the largest proportion of PTEs is concentrated in goethite and amorphous Fe oxyhydroxides and, subordinately, in the low-crystalline chlorite (Figure 7).

Most of the Ni in the studied soils is concentrated in antigorite, magnetite, Cr-magnetite, clinochlore, Fe oxyhydroxides, and low-crystallinity chlorite. The detailed crystallochemical analyses highlighted significant differences in Ni contents, mostly related to the serpentinization degree as well as the textural and structural features. As an example, antigorite crystals occurring in pseudomorphic textures after olivine in soils on PSP have an almost double Ni content compared to those occurring in bastites after pyroxenes, which, on the contrary, show the highest Cr content and a non-negligible amount of other PTEs (particularly Co). This behavior is perfectly consistent with what has been observed recently in a crystallochemical study of parent rocks coming from the same sites investigated in this work [69].

Bulk Ni contents are always much greater in the bedrock (up to 3900 ppm in PSP; [68]) as compared to the soil (down to 275 ppm in A horizon of soil on MS; Table 2) and generally progressively decrease from the C horizon toward the A horizon in all soil types. This trend can be explained by the progressive dissolution of primary Ni-bearing minerals and in particular of olivine (which were detected in trace amounts only in soil profiles on PSP) antigorite, and magnetite whose content systematically decreases as you go upward in the soil profiles (Table 1). Although a significant proportion of the released Ni has been incorporated in amorphous Fe oxyhydroxides and, subordinately, in goethite (only in soils on PSP) and in clay minerals, our data suggest that a non-negligible quantity of nickel has been removed from topsoils during pedogenesis, either leached out from the soil solution or phytoextracted by serpentinophytes (e.g., [77]). As a matter of fact, in our samples, most of the authigenic minerals are represented by amorphous Fe oxyhydroxides that are considered an available source of Ni in soil environments because of their sorption on the surface rather than incorporation within crystal lattice, as for crystalline goethite and hematite (e.g., [23,85,86]).

The bulk soil Cr contents significantly increase from bedrock (Figure 6) toward the top of the profile in soils on PSP, whereas the trend was the opposite in those on MS and FS. This finding agrees well with the mineralogy and mineral chemistry of Cr-bearing minerals that resulted from this work. In soils on PSP, the most important Cr-bearing phases are Cr-spinel, ferrian chromite, and Cr-magnetite, which are considerably less weatherable than magnetite (e.g., [1,2]), the most abundant spinel species within soils on MS and FS. As a matter of fact, they account for about 8–9% of the minerals in soils on PSP (Table 1), whereas the magnetite content systematically decreases upwards in the profiles in the other soil types. Therefore, the Cr enrichment in these soil types appears to be related, at least in part, to a residual enrichment in Cr-spinel, ferrian chromite, and Cr-magnetite due to their very low weatherability in this pedogenic environment. Moreover, Oze et al. [1] reported that chromium(III) would be among the last ions to be removed from the spinel structure compared to other transition elements (such as Fe^{3+}) due to incongruent dissolution, thus progressively enriching

the soil spinels toward Cr-enriched end-members. Nevertheless, Cr variations can be also dependent on oxidation state and pH conditions throughout the soil profile, since the mobility of hexavalent chromium, increases under alkaline conditions.

Based on the above discussion, magnetite, antigorite and clinochlore are more likely sources of chemically mobile Cr in the studied soils. Most of the chromium released during weathering processes appears to be stored in amorphous Fe oxyhydroxides, which contain very high Cr contents (up to 4750 ppm), and, to a lesser extent, in low-crystalline chlorite. As discussed for nickel, the general decrease of bulk soil Cr in the A horizon suggests that these authigenic minerals represent mostly a transient sink, thus a possible source of chemically mobile and bioavailable Cr. This hypothesis is also supported by other studies (e.g., [1,2,23,28]) that indicated that Cr mobility is mostly controlled by the presence and behavior of amorphous Fe oxyhydroxides.

Cobalt is generally present in relatively low concentrations in all soil types and showed contrasting and irregular behavior with respect to both the soil type and depth (Table 2, Figure 6), as observed by other authors (e.g., [87] and references therein). Based on the EPMA and LA–ICP–MS results, the main Co-bearing phases are spinel-group minerals, amorphous Fe oxyhydroxides, and goethite (only in soils on PSP). With respect to studies dealing with Ni and Cr, there are so far few works about cobalt behavior and bioavailability in ultramafic soils (e.g., [28,87–91]). Li et al. [89] proved that plant roots can absorb Co by localized dissolution of amorphous Fe and Mn oxides; based on this assumption and other literature data (e.g., [10,87,90,91]) the amorphous Fe oxyhydroxides detected in the studied soils might be the main phases controlling cobalt distribution and possibly its mobility and bioavailability.

General Environmental Implications

The findings of this work have several implications concerning environmental issues related to the presence of PTEs of geogenic origin as well as for pollution assessment and public government regulations.

Indeed, Cr and Ni in PSP, MS, and FS subsoils and topsoils systematically exceed (up to one order of magnitude) the residential and the industrial threshold values according to Italian law (Figure 8; D.M. 471/1999 [92], D.Lgs 152/2006 [93]). Among the other elements, only Co behavior leads to environmental concern, as shown in Figure 8, having contents above the residential threshold values.

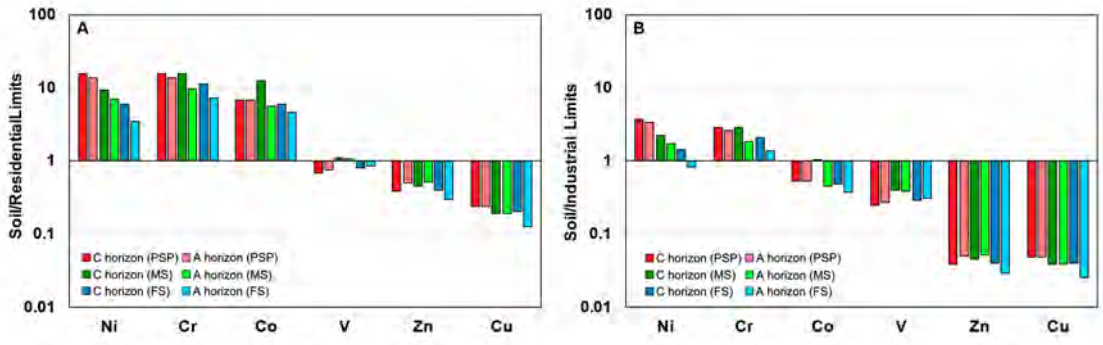

Figure 8. PTEs content normalized to Italian threshold values for residential (**A**) and industrial (**B**) sites according to Italian law (D.M. 471/1999 [92]; D.Lgs 152/2006 [93]).

The results of this multi-analytical approach allowed to demonstrate that the high content of these PTEs are to be considered of geogenic origin since they derive from the natural weathering of parent rocks and from their redistribution during pedogenetic processes. Therefore, they may allow to provide objective basis for setting realistic threshold values based on the evaluation of the geological background, and to exclude possible anthropic contaminations.

Most of the approaches internationally used for pollution assessment are based on the evaluation of soils enrichment factors such as the *Geoaccumulation Index* (e.g., [94]), the *Top Enrichment Factor*

(e.g., [95]) or the *Geochemical Changes Index* (e.g., [79]), the first two based on the variation of PTEs content between topsoil and subsoil, and, the last one on their variation between bedrock and soil profile. Other approaches are based on geostatistical analyses of a large dataset based on regional-scale surveys (e.g., [96] and references therein).

Although geochemical indexes may provide useful general indication on potential contamination of either natural or anthropogenic soils and geostatistical analyses provide a general overview of large areas, these approaches are poorly applicable to very heterogeneous soils, such as those forming on ultramafic bedrocks, which are commonly characterized by significant compositional variation at the regional, local and even site-specific scale.

6. Conclusions

Based on our results, it appears evident that there is a significant relationship between the type of parent rock and the distribution and mobility of PTEs in the studied ultramafic soils, which is clearly related to the degree of serpentinization, which in turn controls the mineralogy and mineral chemistry of primary and authigenic minerals as well as the fate of several trace elements of environmental concern. The release of Cr, Ni, Co, and other PTEs from primary and authigenic minerals into ecosystems during progressive mineral weathering suggests that the different ultramafic soils are a potential source of geogenic metal contamination. This could be intensified in young and poorly developed soils such as those considered in this study.

To have a more complete picture based on the results of this work, further investigation following this approach might involve both different types of ultramafic soils (e.g., those developing on non-serpentinized peridotites) and similar ultramafic soils occurring in different landscapes. Moreover, leaching experiments as well as a multidisciplinary approach involving phyto- and myco-accumulation studies (see, for example, [97–99]) can give a better explanation of the fate of PTEs in young and poorly developed ultramafic soils.

Supplementary Materials: The following are available online at http://www.mdpi.com/2075-163X/9/8/502/s1, Figure S1: Particle size distribution of studied soils according to Folk classification [54], Figure S2: (a): lithorelic in soil on FS bedrock with a micrometric fold marked by unaltered microcrystalline magnetite alignement; (b): alterorelic in soil on PSP bedrock composed by partially altered Cr-spinel within a serpentine + chlorite matrix; (c): alteromorph in soil on MS bedrock composed by completely weathered magnetite aggregates pseudomorphically replaced by cryptocrystalline Fe-oxyhydroxides; (d): enlarged detail of figure S2c; (e) iron crust in soil on PSP bedrock (light gray areas are composed by cryptocrystalline Fe-oxyhydroxides whereas dark gray areas are composed by clay minerals or iddingsitic mixtures); (f) iddingsitic nodules in soils on PSP bedrock. Mineral abbreviations after [67], Table S1: Geographical information of the studied sites (PSP = partially serpentinized peridotite; MS = massive serpentinite; FS = foliated serpentinite), Table S2: Colors code of the soil profiles according to Munsell®Soil Color Charts [53], Table S3: Representative analyses of the main silicates, Table S4: Representative analyses of the spinel-group minerals.

Author Contributions: P.M., L.C., and S.F. conceived of the presented idea; S.F., P.C., A.Z., L.G., and P.M. analyzed the samples and provided data elaboration and curation; P.M., L.C., S.F., P.C., and A.Z. wrote the paper; S.F. made the figures. All authors discussed the results and contributed to the final manuscript.

Funding: This research received no external funding.

Acknowledgments: Synchrotron X-ray diffraction experiments were carried out during beam time allocated for Proposal 20175192/2018 at Elettra Sincrotrone Trieste. Silvia Fornasaro was supported by a University of Genova (Italy) PhD Grant.

Conflicts of Interest: The authors declare no conflict of interest.

References

1. Oze, C.; Fendorf, S.; Bird, D.K.; Coleman, R.G. Chromium geochemistry in serpentinized ultramafic rocks and serpentine soils from the Franciscan complex of California. *Am. J. Sci.* **2004**, *304*, 67–101. [CrossRef]
2. Oze, C.; Fendorf, S.; Bird, D.K.; Coleman, R.G. Chromium geochemistry of serpentine soils. *Int. Geol. Rev.* **2004**, *46*, 97–126. [CrossRef]

3. Burt, R.; Wilson, M.A. Serpentinitic Soils. In *Encyclopedia of Soil Science*, 2nd ed.; Rattan, L., Ed.; Taylor & Francis: Abingdon, UK, 2006; pp. 1564–1567.
4. Rajapaksha, A.U.; Vithanage, M.; Oze, C.; Bandara, W.M.A.T.; Weerasooriya, R. Nickel and manganese release in serpentine soil from the Ussangoda Ultramafic Complex, Sri Lanka. *Geoderma* **2012**, *189–190*, 1–9. [CrossRef]
5. Kelepertzis, E.; Galanos, E.; Mitsis, I. Origin, mineral speciation and geochemical baseline mapping of Ni and Cr in agricultural topsoils of Thiva valley (central Greece). *J. Geochem. Explor.* **2013**, *125*, 56–68. [CrossRef]
6. Rajapaksha, A.; Vithanage, M.; Ok, Y.S.; Oze, C. Cr(VI) formation related to Cr(III)-muscovite and birnessite interactions in ultramafic environments. *Environ. Sci. Technol.* **2013**, *47*, 9722–9729. [CrossRef]
7. Kumarathilaka, P.; Dissanayake, C.; Vithanage, M. Geochemistry of serpentinite soils: A brief overview. *J. Geol. Soc. Sri Lanka* **2014**, *16*, 53–63.
8. Vithanage, M.; Rajapaksha, A.U.; Oze, C.; Rajakaruna, N.; Dissanayake, C.B. Metal release from serpentine soils in Sri Lanka. *Environ. Monit. Assess.* **2014**, *186*, 3415–3429. [CrossRef] [PubMed]
9. Baumeister, J.L.; Hausrath, E.M.; Olsen, A.A.; Tschauner, O.; Adcock, C.T.; Metcalf, R.V. Biogeochemical weathering of serpentinites: An examination of incipient dissolution affecting serpentine soil formation. *Appl. Geochem.* **2015**, *54*, 74–84. [CrossRef]
10. Caillaud, J.; Proust, D.; Philippe, S.; Fontaine, C.; Fialin, M. Trace metals distribution from a serpentinite weathering at the scales of the weathering profile and its related weathering microsystems and clay minerals. *Geoderma* **2009**, *149*, 199–208. [CrossRef]
11. Tashakor, M.; Yaacob, W.Z.W.; Mohamad, H.; Ghani, A.A. Geochemical characteristics of serpentinite soils from Malaysia. *Malays. J. Soil Sci.* **2014**, *18*, 35–49.
12. Kabata-Pendias, A.; Mukherjee, A.B. *Trace Elements from Soil to Human*; Springer-Verlag: Berlin, Germany, 2007; 550p.
13. Kabata-Pendias, A. *Trace Elements in Soils and Plants*, 4th ed.; CRC Press Taylor & Francis Group: Boca Raton, FL, USA, 2011; 505p.
14. Alexander, E.B.; Coleman, R.G.; Keeler-Wolf, T.; Harrison, S. *Serpentine Geoecology of Western North America: Geology, Soils, and Vegetation*; Oxford University Press, Inc.: New York, NY, USA, 2007; 512p.
15. Echevarria, G. Genesis and behaviour of ultramafic soils and consequences for nickel biogeochemistry. In *Agromining: Farming for Metals. Extracting Unconventional Resources Using Plants*; van der Ent, A., Echevarria, G., Baker, A.J.M., Morel, J.L., Eds.; Springer International Publishing: Chan, Switzerland, 2018; pp. 135–156.
16. Cortesogno, L.; Mazzucotelli, A.; Vannucci, R. Alcuni esempi di pedogenesi su rocce ultrafemiche in clima mediterraneo. *Ofioliti* **1979**, *4*, 295–312. (In Italian)
17. Legros, J.P. Soils of alpine mountains. In *Weathering, Soils and Paleosoils: Developments in Earth Surface Processes*, 2nd ed.; Martini, I.P., Chesworth, W., Eds.; Elsevier: Amsterdam, The Netherlands, 1992; pp. 55–181.
18. Morrison, J.M.; Goldhaber, M.B.; Lee, L.; Holloway, J.M.; Wanty, R.B.; Wolf, R.E.; Ranville, J.F. A regional-scale study of chromium and nickel in soils of northern California, USA. *Appl. Geochem.* **2009**, *24*, 1500–1511. [CrossRef]
19. Foth, H.D. *Fundamentals of Soil Science*, 8th ed.; John Wiley & Sons, Inc.: New York, NY, USA, 1991; 272p.
20. Alexander, E.B. Morphology, fertility and classification of productive soils on serpentinised peridotite in California, U.S.A. *Geoderma* **1988**, *41*, 337–351. [CrossRef]
21. Lee, B.D.; Sears, S.K.; Graham, R.C.; Amrhein, C.; Vali, H. Secondary mineral genesis from chlorite and serpentine in an ultramafic soil toposequence. *Soil Sci. Soc. Am. J.* **2003**, *67*, 1309–1317. [CrossRef]
22. Alexander, E.B. Serpentine soil redness, differences among peridotite and serpentinite materials, Klamath Mountains, California. *Int. Geol. Rev.* **2004**, *46*, 754–764. [CrossRef]
23. Chardot, V.; Echevarria, G.; Gury, M.; Massoura, S.; Morel, J.L. Nickel bioavailability in an ultramafic toposequence in the Vosges Mountains (France). *Plant Soil* **2007**, *293*, 7–21. [CrossRef]
24. Hseu, Z.Y.; Tsai, H.; Hsi, H.C.; Chen, Y.C. Weathering sequences of clay minerals in soils along a serpentinitic toposequence. *Clays Clay Miner.* **2007**, *55*, 389–401. [CrossRef]
25. Alexander, E.B. Soil and vegetation differences from peridotite to serpentinite. *Northeast. Nat.* **2009**, *16*, 178–192. [CrossRef]
26. Caillaud, J.; Proust, D.; Righi, D.; Martin, F. Fe-rich clays in a weathering profile developed from serpentinite. *Clays Clay Miner.* **2004**, *52*, 779–791. [CrossRef]

27. Alexander, E.B.; DuShey, J. Topographic and soil differences from peridotite to serpentinite. *Geomorphology* **2011**, *135*, 271–276. [CrossRef]
28. Kierczak, J.; Pędziwiatr, A.; Waroszewski, J.; Modelska, M. Mobility of Ni, Cr and Co in serpentine soils derived on various ultrabasic bedrocks under temperate climate. *Geoderma* **2016**, *268*, 78–91. [CrossRef]
29. Pędziwiatr, A.; Kierczak, J.; Waroszewski, J.; Ratié, G.; Quantin, C.; Ponzevera, E. Rock-type control of Ni, Cr, and Co phytoavailability in ultramafic soils. *Plant Soil* **2018**, *423*, 339–362. [CrossRef]
30. Capponi, G.; Crispini, L. *Note Illustrative della Carta Geologica d'Italia alla scala 1: 50.000 Foglio 213-230, Genova*; APAT, Agenzia per la Protezione dell'Ambiente e per i Servizi Tecnici: Roma, Italy, 2008; 139p.
31. Cimmino, F.; Messiga, B.; Piccardo, G.B. Ti-clinohumite-bearing assemblages within antigoritic serpentinites of the Voltri Massif (Western Liguria): Inferences on the geodynamic evolution of piemontese ultramafic sections. *Ofioliti* **1979**, *4*, 97–120.
32. Messiga, B.; Scambelluri, M. Retrograde *P-T-t* path for the Voltri Massif eclogites (Ligurian Alps, Italy): Some tectonic implications. *J. Metamorph. Geol.* **1991**, *9*, 93–109. [CrossRef]
33. Scambelluri, M.; Müntener, O.; Hermann, J.; Piccardo, G.B.; Trommsdorff, V. Subduction of water into the mantle: History of an Alpine peridotite. *Geology* **1995**, *23*, 459–462. [CrossRef]
34. Federico, L.; Capponi, G.; Crispini, L.; Scambelluri, M.; Villa, I.M. 39Ar/40Ar dating of high-pressure rocks from the Ligurian Alps: Evidence for a continuous subduction–exhumation cycle. *Earth Planet Sc. Lett.* **2005**, *240*, 668–680. [CrossRef]
35. Malatesta, C.; Federico, L.; Crispini, L.; Capponi, G. Fluid-controlled deformation in blueschist-facies conditions: plastic vs brittle behaviour in a brecciated mylonite (Voltri Massif, Western Alps, Italy). *Geol. Mag.* **2018**, *155*, 335–355. [CrossRef]
36. Malatesta, C.; Crispini, L.; Federico, L.; Capponi, G.; Scambelluri, M. The exhumation of high-pressure ophiolites (Voltri Massif, Western Alps): Insights from structural and petrologic data on metagabbro bodies. *Tectonophysics* **2012**, *568*, 102–123. [CrossRef]
37. Capponi, G.; Crispini, L.; Federico, L.; Malatesta, C. Geology of the Eastern Ligurian Alps: A review of the tectonic units. *Ital. J. Geosci.* **2016**, *135*, 157–169. [CrossRef]
38. Rampone, E.; Romairone, A.; Abouchami, W.; Piccardo, G.B.; Hofmann, A.W. Chronology, petrology and isotope geochemistry of the Erro–Tobbio peridotites (Ligurian Alps, Italy): Records of Late Palaeozoic lithospheric extension. *J. Petrol.* **2005**, *46*, 799–827. [CrossRef]
39. Scambelluri, M.; Hoogerduijn Strating, E.H.; Piccardo, G.B.; Vissers, R.L.M.; Rampone, E. Alpine olivine- and titanian clinohumite-bearing assemblages in the Erro–Tobbio peridotite (Voltri Massif, NW Italy). *J. Metamorph. Geol.* **1991**, *9*, 79–91. [CrossRef]
40. Hermann, J.; Muntener, O.; Scambelluri, M. The importance of serpentinite milonite for subduction and exhumation of oceanic crust. *Tectonophysics* **2000**, *327*, 225–238. [CrossRef]
41. Crispini, L.; Capponi, G. Tectonic evolution of the Voltri Group and Sestri Voltaggio Zone (southern limit of the NW Alps): A review. *Ofioliti* **2001**, *26*, 161–164.
42. Capponi, G.; Crispini, L. Structural and metamorphic signature of alpine tectonics in the Voltri Massif (Ligurian Alps, North-Western Italy). *Eclogae Geol. Helv.* **2002**, *95*, 31–42.
43. Federico, L.; Crispini, L.; Scambelluri, M.; Capponi, G. Different PT paths recorded in a tectonic mélange (Voltri Massif, NW Italy): Implications for the exhumation of HP rocks. *Geodin. Acta* **2007**, *20*, 3–19. [CrossRef]
44. Messiga, B.; Piccardo, G.B.; Ernst, W.G. High-pressure eo-Alpine parageneses developed in magnesian metagabbros, Gruppo di Voltri, western Liguria, Italy. *Contrib. Mineral. Petr.* **1983**, *83*, 1–15. [CrossRef]
45. Spandler, C.; Hermann, J.; Faure, K.; Mavrogenes, J.A.; Arculus, R.J. The importance of talc and chlorite "hybrid" rocks for volatile recycling through subduction zones; evidence from the high-pressure subduction mélange of New Caledonia. *Contrib. Mineral. Petr.* **2008**, *155*, 181–198. [CrossRef]
46. Bonifacio, E.; Zanini, E.; Boero, V.; Franchini-Angela, M. Pedogenesis in a soil catena on serpentinite in north-western Italy. *Geoderma* **1997**, *75*, 33–51. [CrossRef]
47. Marsili, S.; Roccotiello, E.; Rellini, I.; Giordani, P.; Barberis, G.; Mariotti, M.G. Ecological studies on the serpentine endemic plant Cerastium utriense Barberis. *Northeast. Nat.* **2009**, *16*, 405–421. [CrossRef]
48. Scopesi, C.; Maerker, M.; Bachofer, F.; Rellini, I.; Firpo, M. Assessment of flash floods in a small Mediterranean catchment using terrain analysis and remotely sensed data: A case study in the Torrente Teiro, Liguria, Italy. *Z. Geomorphol.* **2017**, *61*, 137–163. [CrossRef]

49. Geoportale Regione Liguria. Available online: https://geoportal.regione.liguria.it (accessed on 15 May 2019).
50. Capponi, G.; Crispini, L.; Federico, L.; Cabella, R.; Faccini, F.; Ferraris, F.; Firpo, M.; Marescotti, P.; Piazza, M.; Roccati, A.; et al. *Note illustrative al Foglio 212 'Spigno Monferrato' della Carta Geologica Regionale della Liguria*; Regione Liguria, Dipartimento Ambiente: Genova, Italy, 2013; 144p.
51. Albanese, S.; Sadeghi, M.; Lima, A.; Cicchella, D.; Dinelli, E.; Valera, P.; Falconi, M.; Demetriades, A.; De Vivo, B.; GEMAS Project Team. GEMAS: Cobalt, Cr, Cu and Ni distribution in agricultural and grazing land soil of Europe. *J. Geochem. Explor.* **2015**, *154*, 81–93. [CrossRef]
52. IUSS Working Group WRB. *World Reference Base for Soil Resources 2014, Update 2015. International Soil Classification System for Naming Soils and Creating Legends for Soil Maps*; World Soil Resources Reports No. 106; IUSS Working Group WRB: Rome, Italy, 2015.
53. *Munsell®Soil Color Charts*; Revisised Edition; Munsell Color Company; Kollmorgen Corp.; Macbeth Division: New York, NY, USA, 2000.
54. Folk, R.L. The distinction between grain size and mineral composition in sedimentary-rock nomenclature. *J. Geol.* **1954**, *62*, 344–359. [CrossRef]
55. Schlee, J.S. *Atlantic Continental Shelf and Slope of the United States—Sediment Texture of the Northeastern Part*; Geological Survey Professional Paper 529-L; U.S. Department of the Interior: Washington, DC, USA, 1973; 64p.
56. Delvigne, J. *Atlas of Micromorphology of Mineral Alteration and Weathering*; The Canadian Mineralogy Spec. Publ. 3; Mineralogical Association of Canada: Ottawa, ON, Canada, 1998; 494p.
57. Stoops, G.; Marcelino, V.; Mees, F. (Eds.) *Interpretation of Micromorphological Features of Soils and Regoliths*; Elsevier: Amsterdam, The Netherlands, 2010; 720p.
58. Rebuffi, L.; Plaisier, J.R.; Abdellatief, M.; Lausi, A.; Scardi, P. MCX: A synchrotron radiation beamline for X-ray diffraction line profile analysis. *Z. Anorg. Allg. Chem.* **2014**, *640*, 3100–3106. [CrossRef]
59. Larson, A.C.; Von Dreele, R.B. GSAS. Report No. LAUR 86-748. *J. Appl. Crystallogr.* **2001**, *34*, 210–213.
60. Zucchini, A.; Comodi, P.; Katerinopoulou, A.; Balic-Zunic, T.; McCammon, C.; Frondini, F. Order-disorder-reorder process in thermally treated dolomite samples: A combined powder and single-crystal X-ray diffraction study. *Phys. Chem. Miner.* **2012**, *39*, 219–328. [CrossRef]
61. Frondini, F.; Zucchini, A.; Comodi, P. Water-rock interactions and trace elements distribution in dolomite aquifers: The Sassolungo and Sella systems (Northern Italy). *Geochem, J.* **2014**, *48*, 231–246. [CrossRef]
62. Gentili, S.; Comodi, P.; Nazzareni, S.; Zucchini, A. The Orvieto-Bagnoregio Ignimbrite: Pyroxene crystal-chemistry and bulk phase composition of pyroclastic deposits, a tool to identify syn- and post-depositional processes. *Eur. J. Mineral.* **2014**, *26*, 743–775. [CrossRef]
63. Lafuente, B.; Downs, R.T.; Yang, H.; Stone, N. The power of databases: the RRUFF project. In *Highlights in Mineralogical Crystallography*; Armbruster, T., Danisi, R.M., Eds.; de Gruyter GmbH & Co.: Berlin, Germany, 2015; pp. 1–30.
64. Hill, R.J.; Howard, C.J. Quantitative phase analysis from neutron powder diffraction data using the Rietveld method. *J. Appl. Cryst.* **1987**, *20*, 467–474. [CrossRef]
65. Konta, J. *Theoretical Argillology for the Application of Sealing, Sorbent and Catalytic Clays*; Servizio Publicazioni del Gruppo Italiano dell'AIPEA: Faenza, Italy, 2001; 152p.
66. Petrelli, M.; Morgavi, D.; Vetere, F.; Perugini, D. Elemental imaging and petro-volcanological applications of an improved laser ablation inductively coupled quadrupole plasma mass spectrometry. *Period. Mineral.* **2016**, *85*, 25–39.
67. Kretz, R. Symbols of rock-forming minerals. *Am. Mineral.* **1983**, *68*, 277–279.
68. Zanazzi, P.F.; Comodi, P.; Nazzareni, S.; Andreozzi, G.B. Thermal behaviour of chlorite: An in situ single-crystal and powder diffraction study. *Eur. J. Mineral.* **2009**, *21*, 581–589. [CrossRef]
69. Fornasaro, S.; Comodi, P.; Crispini, C.; Malatesta, C.; Zucchini, A.; Marescotti, P. Potentially toxic elements distribution in the serpentinized and deformed ultramafic rocks from the Voltri Massif (NW, Italy). *Period. Mineral.* **2019**, *88*. [CrossRef]
70. Bani, A.; Echevarria, G.; Zhang, X.; Benizri, E.; Laubie, B.; Morel, J.L.; Simonnot, M.O. The effect of plant density in nickel-phytomining field experiments with Alyssum murale in Albania. *Aust. J. Bot.* **2015**, *63*, 72–77. [CrossRef]
71. Angelone, M.; Vaselli, O.; Bini, C.; Coradossi, N. Pedogeochemical evolution and trace elements availability to plants in ophiolitic soils. *Sci. Total Environ.* **1993**, *129*, 291–309. [CrossRef]

72. Venturelli, G.; Contini, S.; Bonazzi, A.; Mangia, A. Weathering of ultramafic rocks and element mobility at Mt. Prinzera, Northern Apennines, Italy. *Mineral. Mag.* **1997**, *61*, 765–778. [CrossRef]
73. D'Amico, M.; Julitta, F.; Previtali, F.; Cantelli, D. Podzolization over ophiolitic materials in the western Alps (Natural Park of Mont Avic, Aosta Valley, Italy). *Geoderma* **2008**, *146*, 129–137. [CrossRef]
74. Quantin, C.; Ettler, V.; Garnier, J.; Sebek, O. Sources and extractibility of chromium and nickel in soil profiles developed on Czech serpentinites. *C. R. Geosci.* **2008**, *340*, 872–882. [CrossRef]
75. Alves, S.; Trancoso, M.A.; de Lurdes Simões Gonncalves, M.; Correia dos Santos, M.M. A nickel availability study in serpentinised area of Portugal. *Geoderma* **2001**, *164*, 155–163. [CrossRef]
76. Cheng, C.H.; Jien, S.H.; Iizuka, Y.; Tsai, H.; Chang, Y.H.; Hseu, Z.Y. Pedogenic chromium and nickel partitioning in serpentine soils along a toposequence. *Soil Sci. Soc. Am. J.* **2011**, *75*, 659–668. [CrossRef]
77. Bani, A.; Echevarria, G.; Montarges-Pelletier, E.; Gjoka, F.; Sulce, S.; Morel, J.L. Pedogenesis and nickel biogeochemistry in a typical Albanian ultramafic toposequence. *Environ. Monit. Assess.* **2014**, *186*, 4431–4442. [CrossRef] [PubMed]
78. Ratié, G.; Jouvin, D.; Garnier, J.; Rouxel, O.; Miska, S.; Guimarães, E.; Cruz Vieira, L.; Sivry, Y.; Zelano, I.; Montarges Pelletier, E.; et al. Nickel isotope fractionation during tropical weathering of ultramafic rocks. *Chem. Geol.* **2015**, *402*, 68–76. [CrossRef]
79. Kierczak, J.; Neel, C.; Puziewicz, J. Effect of mineralogy and pedoclimatic variations on Ni and Cr distribution in serpentine soils under temperate climate. *Geoderma* **2007**, *142*, 165–177. [CrossRef]
80. Garnier, J.; Quantin, C.; Martins, E.S.; Becquer, T. Solid speciation and availability of chromium in ultramafic soils from Niquelândia, Brazil. *J. Geochem. Explor.* **2006**, *88*, 206–209. [CrossRef]
81. Rabenhorst, M.C.; Foss, J.E.; Fanning, D.S. Genesis of Maryland soils formed from serpentinite. *Soil Sci. Soc. Am. J.* **1982**, *46*, 607–616. [CrossRef]
82. Sawhney, B.L. Interstratification in layer silicates. In *Minerals in Soil Environments*, 2nd ed.; Dixon, J.B., Weed, S.B., Eds.; SSSA Book Series No.1; Soil Science Society of America: Madison, WI, USA, 1989; pp. 789–828.
83. Istok, J.D.; Harward, M.D. Influence of soil moisture on smectite formation in soils derived from serpentinite. *Soil Sci. Soc. Am. J.* **1982**, *46*, 1106–1108. [CrossRef]
84. Yongue-Fouateu, R.; Ghogomu, R.T.; Penaye, J.; Ekodeck, G.E.; Stendal, H.; Colin, F. Nickel and cobalt distribution in the laterites of the Lomié region, south-east Cameroon. *J. Afr. Earth Sci.* **2006**, *45*, 33–47. [CrossRef]
85. Marescotti, P.; Carbone, C.; Comodi, P.; Frondini, F.; Lucchetti, G. Mineralogical and chemical evolution of ochreous precipitates from the Libiola Fe–Cu-sulfide mine (Eastern Liguria, Italy). *Appl. Geochem.* **2012**, *27*, 577–589. [CrossRef]
86. Massoura, S.T.; Echevarria, G.; Becquer, T.; Ghanbaja, J.; Leclerc-Cessac, M.J.L. Control of nickel availability by nickel bearing minerals in natural and anthropogenic soils. *Geoderma* **2006**, *136*, 28–37. [CrossRef]
87. Hsiao, K.H.; Bao, K.H.; Wang, S.H.; Hseu, Z.H. Extractable concentrations of cobalt from serpentine soils with several single-extraction procedures. *Commun. Soil Sci. Plan.* **2009**, *40*, 2200–2224. [CrossRef]
88. Lago-Vila, M.; Arenas-Lago, D.; Rodríguez-Seijo, A.; Andrade Couce, M.L.; Vega, F.A. Cobalt, chromium and nickel contents in soils and plants from a serpentinite quarry. *Solid Earth* **2015**, *6*, 323–335. [CrossRef]
89. Li, Z.; McLaren, R.G.; Metherell, A.K. The availability of native and applied soil cobalt to ryegrass in relation to soil cobalt and manganese status and other soil properties. *New Zealand. J. Agric. Res.* **2004**, *47*, 33–43. [CrossRef]
90. Li, H.-F.; Gray, C.; Mico, C.; Zhao, F.-J.; McGrath, S.P. Phytotoxicity and bioavailability of cobalt to plants in a range of soils. *Geoderma* **2009**, *75*, 979–986. [CrossRef]
91. Tashakor, M.; Yaacob, W.Z.W.; Mohamad, H. Speciation and Availability of Cr, Ni and Co in serpentine soils of Ranau, Sabah. *Am. J. Sci.* **2001**, *2*, 4–9. [CrossRef]
92. Ministerial Decree 25th October 1999 no. 471 - D.M. 471/1999. Regolamento recante criteri, procedure e modalità per la messa in sicurezza, la bonifica e il ripristino ambientale dei siti inquinati ai sensi dell'art. 17 del D.Lgs. 22/97 e successive modificazioni e integrazioni. Gazzetta Ufficiale della Repubblica Italiana 1999, no. 293. Available online: http://www.giaexploring.it/userfiles/files/7.LEGGI_ECT/fl26.pdf (accessed on 19 August 2019).

93. Legislative Decree 3rd April 2006 - D.Lgs 152/2006 - Norme in materia ambientale. Gazzetta Ufficiale della Repubblica Italiana 1999, no. 88. Available online: http://www.isprambiente.gov.it/it/garante_aia_ilva/normativa/normativa-ambientale/Dlgs_152_06_TestoUnicoAmbientale.pdf (accessed on 19 August 2019).
94. Galán, E.; González, I.; Romero, A.; Aparicio, P. A methodological approach to estimate the geogenic contribution in soils potentially polluted by trace elements. Application to a case study. *J. Soils Sediments* **2014**, *14*, 810–818. [CrossRef]
95. Colbourn, P.; Thornton, I. Lead pollution in agricultural soils. *J. Soil Sci.* **1978**, *29*, 513–526. [CrossRef]
96. Reimann, C.; de Caritat, P. Distinguishing between natural and anthropogenic sources for elements in the environment: Regional geochemical surveys versus enrichment factors. *Sci. Tot. Environ.* **2005**, *337*, 91–107. [CrossRef] [PubMed]
97. Marsili, S.; Roccotiello, E.; Carbone, C.; Marescotti, P.; Cornara, L.; Mariotti, M. Plant colonization on a contaminated serpentine site. *Northeast. Nat.* **2009**, *16*, 297–308. [CrossRef]
98. Marescotti, P.; Roccotiello, E.; Zotti, M.; De Capitani, L.; Carbone, C.; Azzali, E.; Mariotti, M.; Lucchetti, G. Influence of soil mineralogy and chemistry on fungi and plants in a waste-rock dump from the Libiola mine (eastern Liguria, Italy). *Period. Mineral.* **2013**, *82*, 141–162.
99. Zotti, M.; Di Piazza, S.; Roccotiello, E.; Lucchetti, G.; Mariotti, M.; Marescotti, P. Microfungi in highly copper-contaminated soils from an abandoned Fe-Cu sulphide mine: Growth responses, tolerance and bioaccumulation. *Chemosphere* **2014**, *117*, 471–476. [CrossRef] [PubMed]